DOI: 10.21062/mft.2025.028 http://www.journalmt.com

A Synthetic Geometric Performance Index for Parts Manufactured by VAT Photopolymerization

Valentina Vendittoli (0000-0001-6332-4203)[1], Wilma Polini (0000-0002-6839-3889)[1], Walter Michael Simon Josef (0009-0005-8787-6666)[2], Giovanni Moroni (0000-0002-7621-3382)[3]
[1]Department of Civil and Mechanical Engineering, Università di Cassino e del Lazio Meridionale, Via Gaetano Di Biasio 43, 03043 Cassino, Italy. E-mail: valentina.vendittoli1@unicas.it; polini@unicas.it
[2]University of Applied Sciences Ansbach, Faculty of Engineering, Residenzstr. 8, 91522 Ansbach, Germany. E-mail: michael.walter@hs-ansbach.de
[3]Mechanical Engineering Department, Politecnico di Milano, Via La Masa 1, 20156 Milano, Italy. E-mail: giovanni.moroni@polimi.it

Geometric deviations play a crucial role in the quality of additive manufacturing, particularly in parts made with biodegradable resins. Accurately controlling dimensional and geometric variations in manufactured components is critical for achieving defect-free production and meeting functional standards. However, defining a final quality score can be challenging due to the numerous dimensional and geometric deviations associated with a part. An innovative metric for evaluating geometric performance was created to measure dimensional precision in components produced through VAT photopolymerization. The index measures the dimensional and geometrical deviations, revealing that external surfaces exhibit greater precision than internal ones. This difference is likely due to internal surfaces overcoming heat dissipation challenges during the cooling process, resulting in less shrinkage for external surfaces. This index is essential in various stages of the manufacturing process, including part design, design for manufacturing and assembly, quality assurance, and process planning, helping to select the appropriate additive manufacturing technology and optimal process parameters.

Keywords: Additive Manufacturing, Geometric Product Specifications, VAT photopolymerization, Biodegradable resin, Performance Index

1 Introduction

Additive Manufacturing (AM) is based on creating 3D components, depositing layer after layer up to reach the desired shape. Unlike subtractive manufacturing, the process is relatively faster and has less material waste production. Considering the state of the used materials, vat photopolymerization, also known as stereolithography (SLA), is the oldest technology; a laser photopolymerized a resin in a liquid state to obtain the final object. Masked stereolithography (MSLA) is an evolution of SLA, and it is faster since each layer is printed all at once [1].

When it comes to 3D printing, polymers are widely used due to their low cost and chemical resistance [2, 3]. In the last decade, different studies have been conducted on vat photopolymerization to discuss the feasibility of using biodegradable biomaterials as a substitute for petroleum derivatives to reduce pollution and their potential application in biomedical fields [4, 5]. They focused their attention on the influence of the resin on the dimensional deviations of the manufactured parts. Each resin has a different colour dye in a suspended form, which might produce different effects on the dimensional behaviour during the printing process [6]. Other studies discuss how different printing positions on the building plate can lead to different results regarding dimensional deviations and deformations of the part geometry. Some build angles are 0°, 45°, and 90° concerning the z-axis. 0° and 45° are widely chosen because the accuracy of printed parts is very high [7]. A parameter connected with the printing direction is the printing time. Specimens that are printed at 0° require less printing time. Some specimens need support to be printed, hence choosing the right build angle leads to low material consumption since 0° minimizes the supports' quantity. The right combination of the build angles and supports can optimize the material consumption and the printing time for the part to be printed [8, 9].

All the works of the literature deal with dimensional or form deviations of the parts manufactured by vat photopolymerization process. Analyzing dimensional and geometric variations in the manufacturing process is essential for producing high-quality parts and assembling them to meet specific functional requirements [10-15]. The considered biodegradable resin is largely used in the biomedical field [16]. Previous works studied benchmark deviation as a function

of printing parameters [17]. Recent works of the authors studied both dimensional and geometric deviations using a Fused Filament Fabrication technique [18, 19] discovering the possibility of analysing a benchmark through a synthetic performance index [20]. An overall performance index was proposed in [21] to take into account mechanical strength and geometric accuracy of the part.

This study aims to contribute to the field of additive manufacturing by introducing an SGPI to evaluate the overall geometric accuracy of parts produced via MSLA using biodegradable resins. While prior research has analyzed either dimensional or geometrical deviations individually, this work uniquely integrates both aspects into a comprehensive metric. By doing so, the SGPI offers a unified approach for assessing part quality, simplifying comparison between different surfaces and parts, and enabling a more informed selection of process parameters and technologies. Moreover, using a customized benchmark geometry to highlight internal and external features allows for a more nuanced understanding of how biodegradable resin behaves under MSLA conditions. This contribution is particularly relevant for sustainable manufacturing and biomedical applications, where precision and environmental impact are critical factors. The printer and resin used were then introduced, along with technical data on the printer and print setup used. The measurement results obtained were compared with the nominal values of the CAD model. A novel synthetic performance index was created, combining all dimensional and geometrical deviations [22] to obtain a single value that can be analysed to define the quality of the benchmark.

2 Material and method

Many existing benchmarks for assessing process capability feature cylindrical elements and protrusions have been made [23]. However, this study emphasizes internal hollows within a part, which present greater challenges in cooling. Additionally, various hollow shapes were included to capture a wide array of geometric deviations. The benchmark proposed in this work is an 80 x 50 x 10 mm rectangular parallelepiped with some holes and slots of different shapes (Fig. 1). The part was created through an MSLA printer, Original Prusa SL1 by Prusa Research (Fig. 2, step: processing).

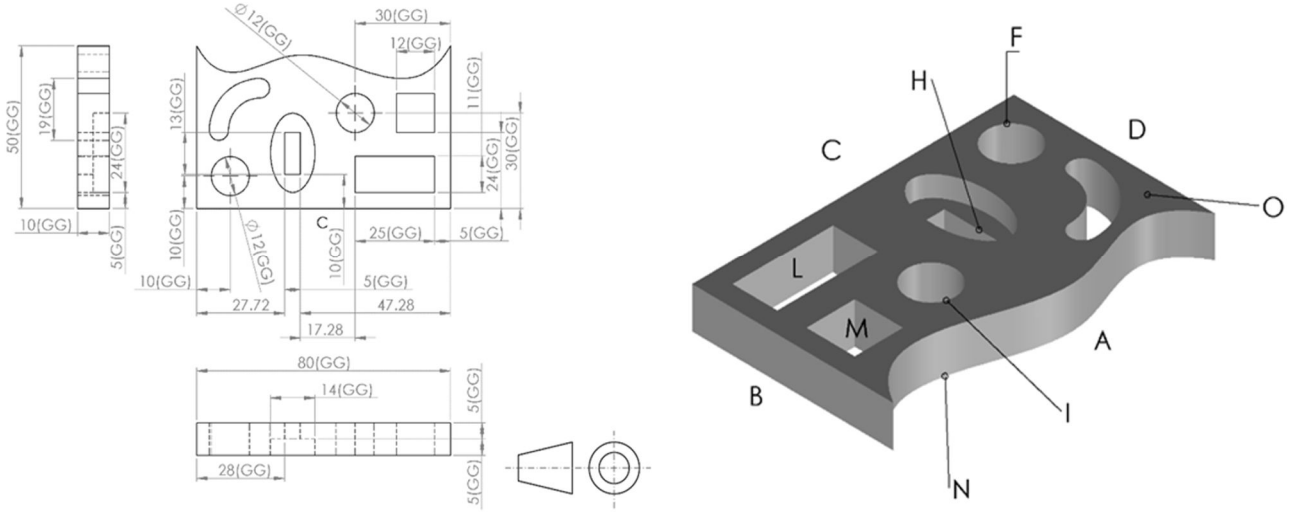

Fig. 1 *Benchmark part: Technical drawing and nominal dimensions (left) and abbreviations of relevant geometrical features (right)*

The vat photopolymerization is a standardized technique based on the photopolymerization of a material in the liquid state, which absorbs heat and hardens thanks to the formation of links in the chemical structure. An evolution of this AM technique is the MSLA. It is called masked because it replies to its original process but uses a different UV light source. Instead of a UV laser, there is an LED array composed of squared pixels under the printing platform that is transparent thanks to a film put underneath. Only the pixels that serve to shape the layer during the printing process are light up. The main advantage is that each layer is polymerized all at once. Furthermore, it is possible to manufacture more than one part for printing without increasing the final printing time.

A biodegradable resin, ANYCUBIC Plant-based UV Resin, was used. Compared to normal liquid resins, this is manufactured from soybean oil. In fact, 45% of the chemical composition is plant-based:

- 45% concentration of Fatty acids, soya, epoxidized, Butyl esters;
- 30% isooctyl acrylate (monomers);
- 15% 2 - [[2,2 - Bis [[(1 - oxalyl) oxy] methyl] butoxy] methyl] - 2 - ethyl - 1,3 - propanediol diacrylate (monomers);

- 5% 2 - hydroxy -1 - (4 - (4 - (2 - hydroxy - 2 - methyl propionyl) benzyl) phenyl) - 2 - methyldopa - 1 - one (photoinitiator);
- 5% colour pigment.

Moreover, the resin can be used at different wavelength ranges, which makes it easy to use with different printers and parameters. Furthermore, it has properties similar to regular resin in a normal environment, but it is compostable if the printed parts are ground and put in a composter [24].

The first step to obtaining the benchmark was preparing the benchmark solid model and exporting it as an STL file. The model was then sliced using Prusa Slicer® software, which positions the part on a virtual build plate, allowing for the adjustment of all printing parameters and simulating the part's creation [25].

At first, two main configurations were analysed to choose each part's optimal position in the buildspace. Since the benchmark was completely flat, laying it down on one side of the build plate without support was better. This reduced the printing time substantially because of fewer layers. Therefore, ten parts were manufactured using parameters suggested by the printer manufacturer [26]. Table 1 provides these details, with layer height specifying the thickness of each printed layer. Furthermore, the exposure time, or duration for which each layer is cured, was defined. Distinct times were set for the initial layer and subsequent layers. Usually, the first layer is cured for more time for good adhesion on the printing platform. Furthermore, an almost completely cured first layer is needed to avoid sagging in the structure during the printing process, since the process is made upside-down.

Usually, SLA parts, once printed, need some post-processing operations. The number of operations increases in this specific case due to the different methodologies. For instance, the printing platform is fully immersed in the resin tank to realize the following layer at each layer. The result is a part with non-polymerized resin residues on the outer surfaces. To remove these, the part is put into a washing tank with isopropyl alcohol for 5 minutes; then dried using hot air for 3 minutes and cured with UV light for 3 minutes in the Prusa CW1 (curing and washing station) (Fig. 2, state: post-processing).

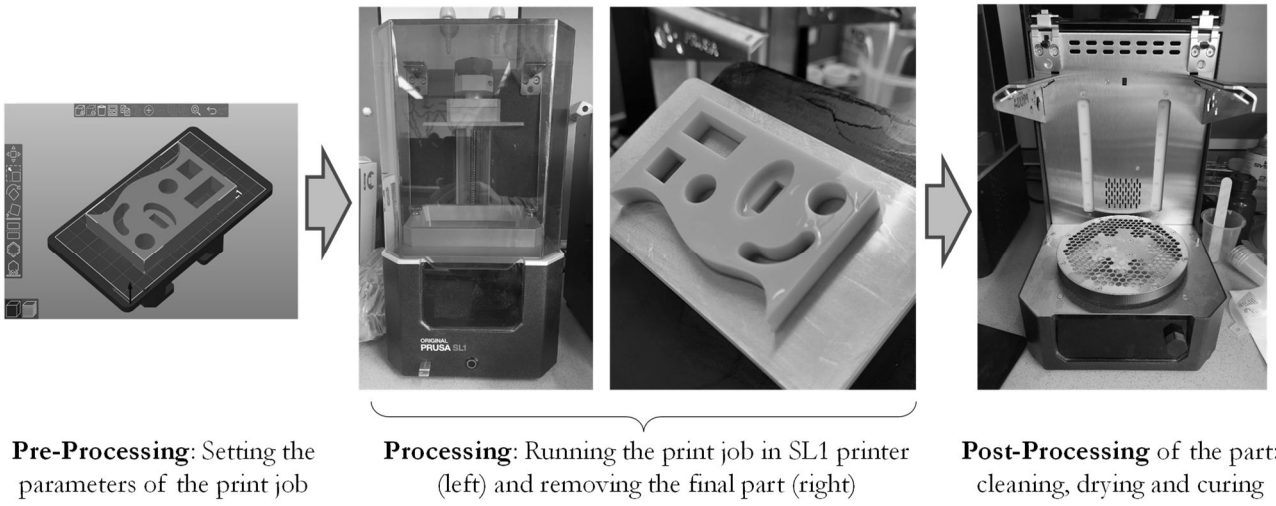

Pre-Processing: Setting the parameters of the print job

Processing: Running the print job in SL1 printer (left) and removing the final part (right)

Post-Processing of the part: cleaning, drying and curing

Fig. 2 *Process from 3D-CAD model to the finished benchmark part*

Tab. 1 *Values of printing parameters set during pre-processing*

Parameter	Value
Print Orientation	0°
Layer Height	0.1 mm
Initial layer height	0.1 mm
Exposure time	13 seconds
Initial exposure time	70 seconds

3 Measurement procedure

A structured light-based coordinate measurement system was employed to evaluate how different printing parameters and resin types impact the dimensional accuracy of the printed parts. This approach captures the object from various angles to reconstruct it as a 3D model. The ATOS Core 200 by GOM (Fig. 3), capable of scanning parts up to 500 mm, was used with a measuring area of 200 x 150 mm and sensor dimensions of 206 x 205 x 64 mm [27]. It captures images from distances up to 250 mm, achieving a maximum resolution of 0.08 mm.

For the measurement process, fringe patterns are projected onto the part's surfaces and recorded by two cameras functioning on the Triple Scan Principle.

The measurement began with preparing each part individually. Aedrox NQ1 spray was applied to create a matte finish, reducing light reflections and enhancing scan quality. Markers were placed on each part's surface, which the camera automatically detected during scanning, facilitating precise alignment. Once prepared, the part was positioned on a swivel plate to initiate the image capture process (Fig. 3). GOM Scan software was utilized to capture images and convert them into 3D representations of the measured part. The software automatically calculates the photograms and generates a 3D mesh of the part.

GOM Inspect software [28] was employed to compare the nominal STL model with the measured STL version. The nominal and measured solid models were registered using the Gaussian best-fit method (Fig. 3, mapping). Once registered, the measured clouds of points were elaborated through the least squares algorithm to estimate the dimensional and geometrical deviations from the nominal (Fig. 3, measurements).

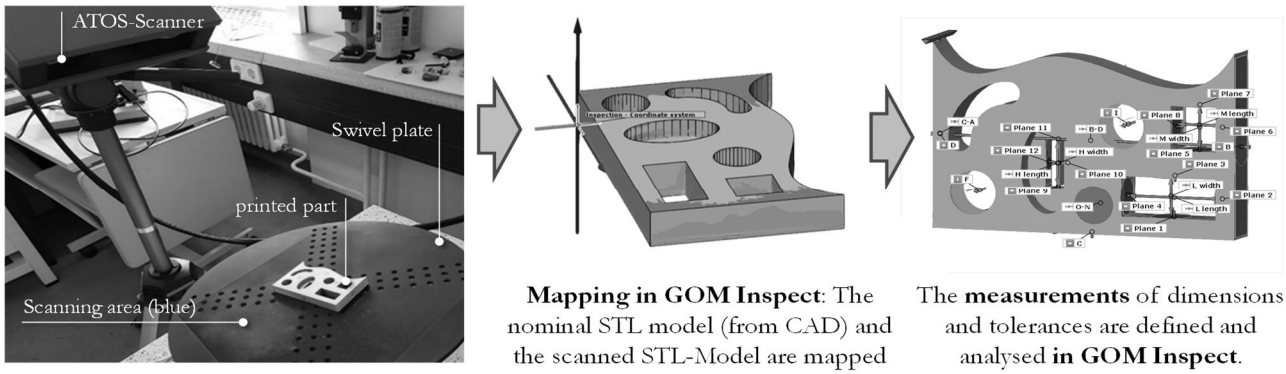

Mapping in GOM Inspect: The nominal STL model (from CAD) and the scanned STL-Model are mapped

The **measurements** of dimensions and tolerances are defined and analysed **in GOM Inspect**.

Fig. 3 *Image Capturing Setup and further processing of the resulting point-could-based STL model of the scanned part*

4 Results

At first, the maximum, minimum, and average values and the standard deviation were calculated for the dimensions of the printed parts. In Fig. 1 (right) all the features that were considered for the analysis are shown. The percentage difference between the mean measurement and the nominal dimension was calculated for each feature:

$$\text{Variation} = \frac{\mu - \text{Nominal}}{\text{Nominal}} \cdot 100\ \%, \qquad (1)$$

Where:

μ…The average/mean of the measured value of each dimension.

Tab. 2 *Measurement results of dimensions (μ = mean; σ = standard deviation)*

Measurement	μ in mm	σ in mm	Nominal value in mm	Variation in %
Distance B-D	80.037	0.030	80	+0.05%
Length D	50.032	0.009	50	+0.06%
Distance O-N	10.019	0.006	10	+0.19%
Diameter cylinder F	11.932	0.022	12	-0.57%
Diameter cylinder I	11.939	0.020	12	-0.51%
Length H	12.966	0.042	13	-0.26%
Width H	4.976	0.062	5	-0.49%
Length M	11.918	0.027	12	-0.68%
Width M	11.888	0.030	12	-0.93%
Width L	24.864	0.036	25	-0.54%
Length L	11.034	0.035	11	+0.31%

It can be noticed that the dimensions differ very little from the nominal between -0.93% to +0.31%. The results in Table 2 indicate that external surfaces are more accurate than internal ones. The percentage variations range from 0.05% to 0.19% for external surfaces and -0.93% to +0.31% for internal surfaces. Moreover, the geometrical deviations were evaluated (see Table 3). The average value of cylindrical surfaces ranges from 0.017 mm to 0.579 mm, with a standard deviation of 0.008 mm up to 0.066 mm. In comparison, the average value of plane surfaces ranges from 0.072 mm to 0.469 mm, with a standard deviation of 0.009 mm up to 0.131 mm. The observed dimensional and geometric discrepancies in parts produced with biodegradable resin are similar to those in non-biodegradable resin under the same manufacturing technology.

Tab. 3 *Measurement results of geometrical deviations (μ = mean; σ = standard deviation)*

Measurement	Maximum in mm	Minimum in mm	μ in mm	Range in mm	σ in mm
Parallelism L	0.326	0.164	0.251	0.162	0.048
Perpendicularity L	0.092	0.060	0.072	0.032	0.009
Position L	0.566	0.209	0.381	0.357	0.112
Perpendicularity M	0.109	0.057	0.076	0.052	0.019
Parallelism M	0.189	0.124	0.143	0.065	0.023
Position M	0.670	0.280	0.469	0.390	0.131
Perpendicularity H	0.357	0.154	0.243	0.203	0.058
Parallelism H	0.396	0.244	0.328	0.152	0.058
Perpendicularity F-N	0.036	0.008	0.017	0.028	0.008
Perpendicularity F-O	0.037	0.010	0.019	0.027	0.008
Cylindricity F	0.145	0.112	0.130	0.033	0.012
Position I	0.698	0.513	0.579	0.185	0.066
Perpendicularity I-N	0.044	0.015	0.024	0.029	0.009
Perpendicularity I-O	0.040	0.004	0.022	0.036	0.009
Cylindricity I	0.130	0.104	0.115	0.026	0.009
Perpendicularity C-B	0.278	0.106	0.205	0.172	0.056
Perpendicularity N-B	0.283	0.144	0.211	0.139	0.041
Perpendicularity O-B	0.236	0.185	0.208	0.051	0.016
Perpendicularity N-C	0.253	0.111	0.204	0.142	0.050
Perpendicularity O-C	0.231	0.112	0.202	0.119	0.046
Parallelism B-D	0.480	0.305	0.390	0.175	0.064
Perpendicularity C-D	0.238	0.111	0.168	0.127	0.039
Perpendicularity N-D	0.323	0.184	0.250	0.139	0.045
Perpendicularity O-D	0.309	0.149	0.225	0.160	0.050
Flatness B	0.385	0.339	0.368	0.046	0.018
Flatness C	0.409	0.365	0.389	0.044	0.021
Flatness D	0.379	0.327	0.346	0.052	0.020
Flatness N	0.517	0.373	0.446	0.144	0.050
Flatness O	0.372	0.323	0.348	0.049	0.020
Parallelism O-N	0.416	0.357	0.382	0.059	0.019

5 Discussion

A large number of dimensional and geometrical deviations were collected for the printed parts and generally are collected industrially for the manufactured workpieces; so, it was looked for a way to combine these evaluations in a unique synthetic performance index that summarizes the quality of the part. It was calculated a Synthetic Geometrical Performance Index by combining the dimensional and geometrical deviations, which was considered independent, in such a way:

$$\mathbf{SGPI_{Surface}} = \sqrt{\sum_{i=1}^{n} DR_i^{\,2}}\ \mathbf{[mm]}, \qquad (2)$$

Where:

DR_i…The i-th dimensional or geometrical deviation related to the manufactured surface among its n-deviations, such as a dimensional deviation from nominal, a flatness or cylindricity deviation, and so on. Each i-th deviation was assessed by calculating the range between maximum and minimum values for dimensions and using average values for geometric deviations. A higher SGPI value indicates lower accuracy of the manufactured surface, while a lower value reflects improved feature quality.

The average SGPI for a surface was determined by dividing its SGPI value by the total number of contributions, allowing for a straightforward assessment of each contribution:

$$\mathrm{SGPI_{Surface_{Avg}}} = \frac{\mathrm{SGI_{Surface}}}{n}\ [\mathrm{mm}], \qquad (3)$$

Table 4 presents the results for each manufactured part's surface, with $SGPI_{Surface}$ values varying between 0.152 mm and 0.643 mm, and average SGPI values spanning from 0.038 mm to 0.446 mm. Ultimately, the SGPI for each manufactured part, as listed in Table 5, was computed to indicate each part's quality.

$$\mathrm{SGPI_{Part}} = \sqrt{\sum_{j=1}^{m}\sum_{i=1}^{n} DR_{ij}^{\,2}}\ [\mathrm{mm}], \qquad (4)$$

Where:

DR_{ij}…The i-th deviation associated with the j-surface of the manufactured part.

The results in Table 5 show a stable printing process with a 12% variation throughout the printing parts.

Tab. 4 *SGPI (reading instruction: "the smaller the index, the higher is the accuracy/quality"; W and L are respectively width and length; the used symbols for the geometrical tolerances are following the symbols applied in GD&T standards from ISO and DIN)*

Surface	Dimensional and geometrical deviations in mm						$SGPI_{Surface}$ [mm]	$SGPI_{SurfaceAvg}$ [mm]
D	W 0.02	∥B 0.39	⊥C 0.16	⊥N 0.25	⊥O 0.23	▱ 0.35	0.643	0.107
B	L 0.09	⊥C 0.2	⊥N 0.21	⊥O 0.21	▱ 0.37		0.522	0.104
C		⊥N 0.20	⊥O 0.20	▱ 0.39			0.483	0.161
N			▱ 0.45				0.446	0.446
O	L 0.02	▱ 0.38	∥N 0.35				0.517	0.172
F	Ø 0.08	⌭ 0.13	⊥N 0.02	⊥O 0.02			0.152	0.038
I	Ø 0.06	⌭ 0.12	⊥N 0.02	⊥O 0.02	⌖ 0.58		0.594	0.119
H	L 0.10	W 0.18	∥12 0.33	⊥11 0.24			0.458	0.115
M	L 0.01	W 0.08	∥8 0.14	⊥7 0.08	⌖ 0.05		0.502	0.100
L	L 0.12	W 0.12	∥1 0.25	⊥4 0.07	⌖ 0.38		0.492	0.099

Tab. 5 *$SGPI_{Part}$*

Benchmark part number	$SGPI_{Part}$ [mm]
1	1.67
2	1.65
3	1.42
4	1.63
5	1.43
6	1.65
7	1.59
8	1.65
9	1.47
10	1.54

6 Conclusion

This study advances the field of sustainable additive manufacturing by applying a SGPI to parts produced via MSLA using a biodegradable, plant-based resin. The goal is to evaluate, with the use of MSLA technology, the dimensional and geometric deviations in parts fabricated from biodegradable resin.

The experimental results reveal that external surfaces exhibit higher precision than internal ones, with dimensional deviations ranging from +0.05% to +0.19% externally and –0.93% to +0.31% internally. This trend is likely caused by reduced heat dissipation in internal features during curing. Geometrical deviations were found relevant, spanning from 0.017 mm to 0.579 mm, with results comparable to those obtained using conventional, non-biodegradable resins under similar conditions. To express the quality of the part produced by MSLA, a synthetic geometrical performance index (SGPI) was introduced. The part's quality increases as its value decreases.

The SGPI effectively consolidates numerous dimensional and geometric deviations into one metric, enabling simplified evaluation and direct comparison of part quality. This index provides a practical tool for identifying critical surfaces, optimizing printing parameters, and guiding technology selection in design and process planning.

Beyond characterizing part quality, the SGPI enables data-driven optimization of additive manufacturing processes, supporting decision-making throughout the product development cycle. It has the potential to be employed not only in quality control but also early in the design phase, in alignment with design for manufacturing, assembly, and sustainability goals.

Future work will validate the SGPI's generalizability across different AM technologies, resins, and parameter sets to confirm its effectiveness in broader industrial applications [22].

Declarations

Conflict of interests. The authors declare that they have no known competing financial interests or personal relationships that could have appeared to influence the work reported in this paper.

References

[1] STANSBURY, J.W. AND IDACAVAGE, M.J. (2016) "3D printing with polymers: Challenges among expanding options and opportunities", *Dental Materials*, 32(1), pp. 54–64. Available at: https://doi.org/10.1016/j.dental.2015.09.018.

[2] SABBATINI, B., CAMBRIANI, A., CESPI, M., PALMIERI, G., PERINELLI, D.R. AND BONACUCINA, G. (2021) "An overview of natural polymers as reinforcing agents for 3D printing", *Chem Engineering*, 5(4), p. 78. Available at: https://doi.org/10.3390/chemengineering5040078.

[3] SEDLAK, J., JOSKA, Z., HRBÁČKOVÁ, L., JURICKOVA, E., HRUŠECKÁ, D. AND HORAK, O. (2022) "Determination of Mechanical Properties of Plastic Components Made by 3D Printing", *Manufacturing Technology*, 22(6), pp. 733–746. Available at: https://doi.org/10.21062/mft.2022.082.

[4] MONDAL, D., HAGHPANAH, Z., HUXMAN, C.J., TANTER, S., SUN, D., GORBET, M. AND WILLETT, T.L. (2021) "mSLA-based 3D printing of acrylated epoxidized soybean oil - nano-hydroxyapatite composites for bone repair", *Materials Science and Engineering: C*, 130, p. 112456. Available at: https://doi.org/10.1016/j.msec.2021.112456.

[5] BAO, L., BIAN, L., ZHAO, M., LEI, J. AND WANG, J. (2014) "Synthesis and self-assembly behavior of a biodegradable and sustainable soybean oil-based copolymer nanomicelle", *Nanoscale Research Letters*, 9(1). Available at: https://doi.org/10.1186/1556-276x-9-391.

[6] TULCAN, A., VASILESCU, M.D. AND TULCAN, L. (2021) "Comparative study of the influence of Bio-Resin color on the dimension, flatness and straightness of the part in the 3D printing process", *Polymers*, 13(9), p. 1412. Available at: https://doi.org/10.3390/polym13091412.

[7] MATUŠ, M., BECHNÝ, V., JOCH, R., DRBÚL, M., HOLUBJÁK, J., CZÁN, A., NOVÁK, M. AND SAJGALIK, M. (2023) "Geometric Accuracy of Components Manufactured by SLS Technology Regarding the Orientation of the Model during 3D Printing", *Manufacturing Technology,* 23(2), pp. 233–240. Available at: https://doi.org/10.21062/mft.2023.027.

[8] RUBAYO, D.D., PHASUK, K., VICKERY, J.M., MORTON, D. AND LIN, W. (2021) "Influences of build angle on the accuracy, printing time, and material consumption of additively manufactured surgical templates", *Journal of Prosthetic Dentistry*, 126(5), pp. 658–663. Available at: https://doi.org/10.1016/j.prosdent.2020.09.012.

[9] HADA, T., KANAZAWA, M., IWAKI, M., ARAKIDA, T., SOEDA, Y., KATHENG, A., OTAKE, R. AND MINAKUCHI, S. (2020) "Effect of printing direction on the accuracy of 3D-Printed dentures using stereolithography technology", *Materials*, 13(15), p. 3405. Available at: https://doi.org/10.3390/ma13153405.

[10] POLINI, W. AND CORRADO, A. (2016) "Geometric tolerance analysis through Jacobian model for rigid assemblies with translational deviations", *Assembly Automation*, 36(1), pp. 72–79. Available at: https://doi.org/10.1108/aa-11-2015-088.

[11] CORRADO, A. AND POLINI, W. (2019) "Measurement of high flexibility components in composite material by touch probe and force sensing resistors", *Journal of Manufacturing Processes*, 45, pp. 520–531. Available at: https://doi.org/10.1016/j.jmapro.2019.07.038.

[12] CARRINO, L., GIORLEO, G., POLINI, W. AND PRISCO, U. (2002) "Dimensional errors in longitudinal turning based on the unified generalized mechanics of cutting approach", *International Journal of Machine Tools & Manufacture*, 42(14), pp. 1517–1525. Available at: https://doi.org/10.1016/s0890-6955(02)00118-9.

[13] CORRADO, A., POLINI, W. AND MORONI, G. (2017) "Manufacturing signature and operating conditions in a variational model for tolerance analysis of rigid assemblies", *Research in Engineering Design*, 28(4), pp. 529–544. Available at: https://doi.org/10.1007/s00163-017-0250-y.

[14] CORRADO, A. AND POLINI, W. (2016) "Assembly design in aeronautic field: From assembly jigs to tolerance analysis", *Proceedings of the Institution of Mechanical Engineers, Part B: Journal of Engineering Manufacture*, 231(14), pp. 2652–2663. Available at: https://doi.org/10.1177/0954405416635033.

[15] ALEXOPOULOU, V., CHRISTODOULOU, I. AND MARKOPOULOS, A. (2024) "Investigation of Printing Speed Impact on the Printing Accuracy of Fused Filament Fabrication (FFF) ABS Artefacts", *Manufacturing Technology,* 24(3), pp. 333–337. Available at: https://doi.org/10.21062/mft.2024.042.

[16] GROHMANN, P. AND WALTER, M.S.J. (2021) "Speeding up statistical tolerance analysis to real time", *Applied Sciences*, 11(9), p. 4207. Available at: https://doi.org/10.3390/app11094207.

[17] RUPAL, B.S., AHMAD, R. AND QURESHI, A.J. (2018) "Feature-Based methodology for design of geometric benchmark test artifacts for additive manufacturing processes", *Procedia CIRP*, 70, pp. 84–89. Available at: https://doi.org/10.1016/j.procir.2018.02.012.

[18] POLINI, W. AND CORRADO, A. (2023) "Dimensional and geometrical deviations of an assembly with a lattice structure manufactured by a material extrusion process: numerical and experimental results", *The International Journal of Advanced Manufacturing Technology*, 127(1–2), pp. 689–701. Available at: https://doi.org/10.1007/s00170-023-11579-8.

[19] POLINI, W. AND CORRADO, A. (2024) "A design for additive manufacturing tool for parts obtained through a material extrusion process", *Progress in Additive Manufacturing*, 9, pp. 285–298. Available at: https://doi.org/10.1007/s40964-023-00451-6.

[20] VENDITTOLI, V., POLINI, W. AND WALTER, M.S.J. (2022) "Geometrical deviations of green parts due to additive manufacturing: a synthetic geometrical performance index", *Procedia CIRP*, 114, pp. 159–164. Available at: https://doi.org/10.1016/j.procir.2022.10.036.

[21] VENDITTOLI, V., POLINI, W. AND WALTER, M.S.J. (2023) "An overall performance index to quantify dimensional accuracy and mechanical strength of parts manufactured through VAT photopolymerization in biodegradable and non-biodegradable resin", *The International Journal of Advanced Manufacturing Technology*, 128(11–12), pp. 5491–5502. Available at: https://doi.org/10.1007/s00170-023-12285-1.

[22] WALTER, M.S.J. (2019) "Dimensional and Geometrical Tolerances in Mechanical Engineering – a Historical Review", *Machine Design*, 11(3), pp. 67–64. Available at: https://doi.org/10.24867/MD.11.2019.3.67-74.

[23] REBAIOLI, L. AND FASSI, I. (2017) "A review on benchmark artifacts for evaluating the geometrical performance of additive manufacturing processes", *The International Journal of Advanced Manufacturing Technology*, 93(5–8), pp. 2571–2598. Available at: https://doi.org/10.1007/s00170-017-0570-0.

[24] *ANYCUBIC PLANT-BASED UV RESIN* (2020) *ANYCUBIC-US*. Available at: https://www.anycubic.com/collections/plant-based-uv-resin/products/anycubic-plant-based-uv-resin (Accessed: October 4, 2023).

[25] *PRUSASLICER | ORIGINAL PRUSA 3D PRINTERS DIRECTLY FROM JOSEF Prusa* (2023) *Prusa3D by Josef Prusa*. Available at: https://www.prusa3d.com/page/prusaslicer_424/ (Accessed: October 4, 2023).

[26] *ISO/ASTM 52902:2019* (2019) *ISO*. Available at: https://www.iso.org/standard/67287.html (Accessed: October 4, 2023).

[27] *3D SCANNER ATOS* (2020) *GOM ATOS*. Available at: https://www.gom.com/en/products/3d-scanning/atos-core#main-content (Accessed: October 4, 2023).

[28] *GOM INSPECT SOFTWARE* (2020) *GOM ATOS*. Available at: https://www.gom.com/en/products/zeiss-quality-suite/gom-inspect-pro (Accessed: October 4, 2023).